A Three-Dimensional Model of the Lithosphere Dynamics, Seismicity Structure, and Variations in the Caspian Sea Level

V. I. Ulomov

Schmidt United Institute of Physics of the Earth, Russian Academy of Sciences,
Bol'shaya Gruzinskaya ul. 10, Moscow, 123995 Russia
Received December 12, 2002

Abstract—Based on the analysis of the deep structure and dynamics of the lithosphere, as well as the study of the regional seismicity pattern and recent tectonic movements, this paper presents a 3-D seismogeodynamic model of the Caspian region according to which a seismic activation is preceded by the upwarping of the southern Caspian seafloor and the appearance of "excessive" sea water and, vice versa, a general sea level decrease is observed after large earthquakes and subsidence of associated crustal areas in the subduction zone. Numerical estimates are obtained for geodynamic deformations in the southern Caspian oceanic lithosphere responsible for the accumulation of elastic stresses and preseismic processes of local earthquakes. Examination of variations in the seismic regime and Caspian Sea level revealed regular patterns supporting a common origin of both phenomena. Being isolated from oceans, the Caspian basin is shown to be very sensitive even to minor deformations of the lithosphere and can be regarded as an indicator of the local geodynamics and seismicity. Joint studies of seismo- and hydrogeodynamic phenomena provide new possibilities for the long-term prediction of strong earthquakes in the Caspian region.

INTRODUCTION

The Caspian region is unique in many respects. The Caspian Sea is abundant in natural resources and thereby attracts the attention of both scientists and statesmen. This region is characterized by a very high geodynamic and seismic activity, which makes it seismically hazardous. The strongest earthquakes with magnitudes of 8.0 and higher are known to have occurred on the southern, western, and eastern coasts of the Caspian Sea. The occurrence of seismic sources at fairly great depths in its central part is evidence of seismogeodynamic processes due to the interaction of lithospheric plates along the Cheleken–Apsheron relict subduction zone [Ulomov, 1993, 1997]. The tsunami phenomena often observed here also make this region resemble similar oceanic structures [Dotsenko *et al.*, 2001, 2002]. Another, even more convincing evidence of relict subduction zones in the Iran–Caucasus–Anatolia region is the seismically active arc of the Zagros Mountains and the Persian Gulf (the former forearc basin). On the other hand, the Caspian Sea is advantageously distinguished from other, "classical" subduction zones. As it is isolated from oceans, its water level is sensitive to even minor regional or local deformations, which makes it a specific indicator of the regional geodynamics and local seismicity.

The problem of anomalous variations in the Caspian Sea level, being significant in both scientific and practical aspects, has been widely discussed [Shilo *et al.*, 1989; Vdovykin, 1990; Golubov, 1994; Lilienberg, 1994; Ulomov, 1997; Golubov *et al.*, 1998; Ulomov *et al.*, 1999, 2002; Lavrushin *et al.*, 2001; Leonov *et al.*, 2001; Ivanova and Trifonov, 2002; Jackson *et al.*, 2002]. Various schemes of active tectonics were proposed for the Caspian region and the South Caspian basin (e.g., see [Kaban *et al.*, 1998; Guliev *et al.*, 2002; Jackson *et al.*, 2002]), but, to the best of my knowledge, no physical model quantifying the seismogeodynamic and hydrogeological processes in the region has been developed.

Based on the systematization and analysis of geological, seismological, and other geophysical data, as well as the study of the deep structure and regional seismicity, a seismogeodynamic model providing new insights into anomalous Caspian Sea level variations in relation to the geodynamics and seismicity of the region is proposed below.

DEEP STRUCTURE OF THE CASPIAN REGION

In accordance with its deep structure, the Caspian Sea divides into northern, central, and southern parts. In the seismogeodynamic respect, most interesting is the deep structure of the central Caspian region, which is the zone of active junction of the Caucasus–Kopet Dag Alpine geological structure and the Scythian-Turan epi-Hercynian platform (Fig. 1). This zone, separating the southern and northern Caspian regions, is traceable by the trans-Caspian Cheleken-Apsheron threshold, as well as by a narrow band of local earthquake sources and maximum gradients of isostatic gravity anomalies, magnetic field, heat flux, and other geophysical fields. The topography gradient of the consolidated crust surface is well observable from the Great Balkhan Ridge in the east to the Derbent basin (inclusive) in the west.
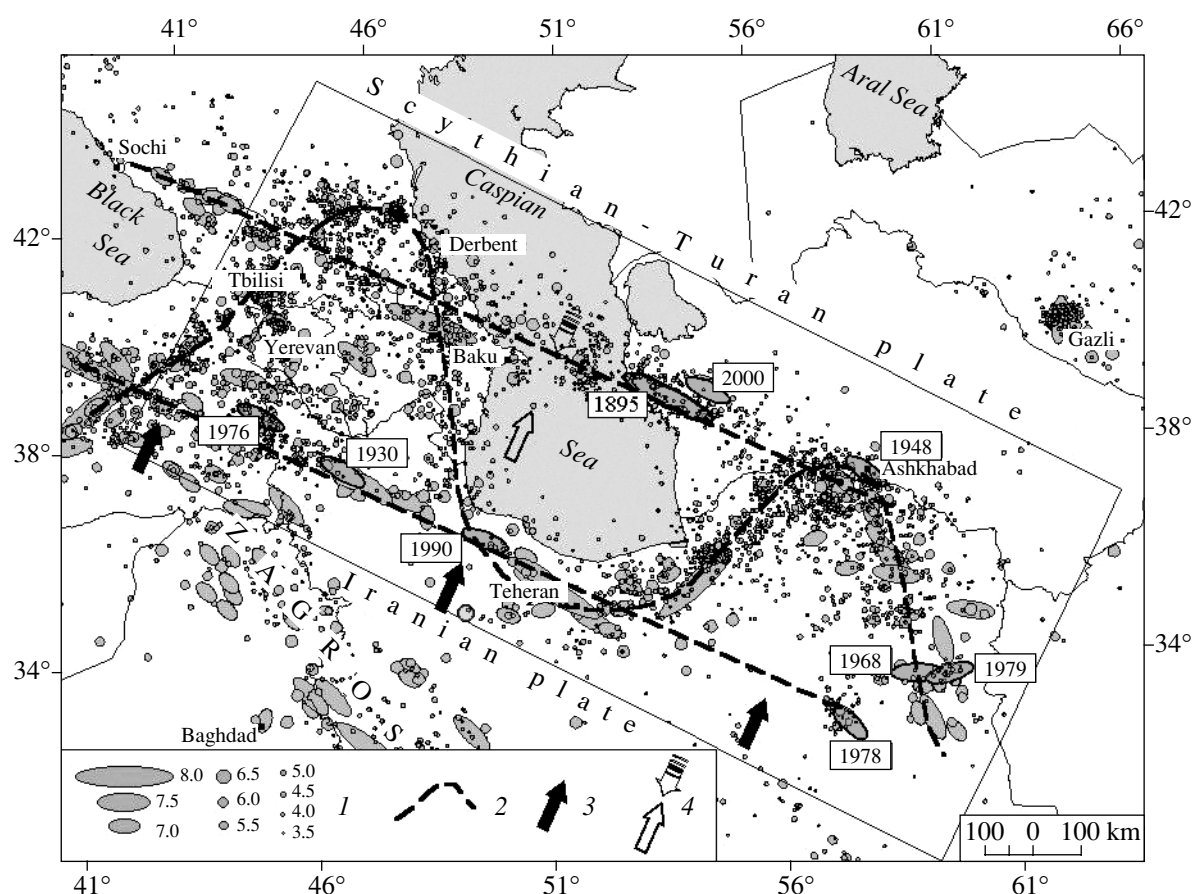
Fig. 1. Seismicity of the Caspian Sea and adjacent areas: (*1*) sources of known earthquakes of different magnitudes (sources with $M = 7.0 \pm 0.2$, 7.5 ± 0.2, and 8.0 ± 0.2 are shown as ellipses reflecting their horizontal sizes and orientations; sources with magnitudes $M = 6.5 \pm 0.2$ and lower are shown as symbolic circles of decreasing diameter); (*2*) axes of structured seismicity; (*3*) direction of the pressure exerted by the Arabian and Iranian plates; (*4*) direction of the movement of the South Caspian oceanic plate and the response of the North Caspian continental lithosphere. The rectangle is the study region. The source of the Krasnovodsk $M = 8.0$ earthquake and the sources of the $M = 7.5 \pm 0.2$ earthquakes that occurred after the 150-year absence of such events in the region are marked by ellipses with thicker outlines, with indication of their occurrence years (see also Fig. 7).

The Caspian Sea depth is no more than 2–4 m in the north and is about 1200 m in the south.

The first studies of the Caspian crust using deep seismic sounding (DSS) were conducted in 1956 by Galperin *et al.* [1962], who revealed anomalously high *P* wave velocities (about 6.5 km/s) and were first to ascribe the central and southern Caspian crust to the suboceanic type, based on structural constraints. This crust was also found to extend beyond the Caspian Sea water area at its eastern coast, south of the Great Balkhan Ridge.

According to DSS data, the crystalline basement surface under the Cheleken-Apsheron threshold abruptly plunges southward from depths of 2–3 km to 20 km and more. The platform territory, both on land and in the northern Caspian Sea, has a typically continental crust under a thin (2–3 km) sedimentary cover consisting of "granitic" (about 10 km thick) and "basaltic" (15–20 km) layers and characterized by positive gravity anomalies. The crustal base (Moho) dips toward the Caucasus and Kopet Dag to depths of 45–50 km and more. As noted above, the crust of the South Caspian basin is oceanic and consists of a thick (over 20 km) sedimentary sequence and a basaltic layer 10–15 km thick. No granitic layer is present here (which is typical of the oceanic lithosphere). The Moho depth under the basin is 30–35 km, and high negative gravity anomalies are observed in the region. The sedimentary cover is strongly faulted and folded along the Cheleken-Apsheron threshold, which is additional evidence for intense dynamics of the seafloor here due to subduction processes [Ulomov, 1993, 1997; Ulomov *et al.*, 1999, 2002].

The original DSS results obtained in the middle of the past century were recently revised and were nearly completely confirmed [Baranova *et al.*, 1990]. In particular, the South Caspian basin was demonstrated once more to have a crust differing from adjacent platform areas. Modern data processing methods significantly increased the velocity structure resolution of the sedi-

mentary cover and provided more detailed constraints on the Moho topography within the basin. Also confirmed were anomalously low velocities in the thick sedimentary sequence, indicating its large porosity despite the high pressures and temperatures at depths of 15–20 km. Two lower-velocity layers have been discovered at these depths and in the sedimentary cover at depths of 7 to 12 km. The origin of the upper layer is interesting from the standpoint of geodynamics because it includes mud volcano sources [Baranova *et al.*, 1990; Panakhi and Rakhmanov, 2000]. The deeper layer with P velocities that are very low for such depths (about 4 km/s) is also anomalous.

The most recent geophysical studies showed that the structure of the South Caspian basin crust is consistent with typical characteristics of other deep sedimentary basins, but is characterized by a more intense process of crustal shortening. Thus, low seismic velocities in sediments can indicate rapid downwarping of the consolidated basement that is not accommodated by an appropriate increase in the density of the sedimentary cover [Baranova *et al.*, 1990]. This conclusion is supported by the isostatic disbalance of the lithosphere under the South Caspian basin. Another factor in favor of its dynamics is the contemporary seismic activity along edges of the oceanic lithosphere block (the presence of subcrustal seismic sources at its boundary with the platform, mud volcanism, higher electrical conductivity layers in the upper mantle, etc.)

SEISMICITY STRUCTURE

In this work, the seismicity pattern and seismic regime were studied within the area including genetically related lithospheric structures of the eastern Caucasus, Elburz, Kopet Dag, and the Caspian Sea (Fig. 1). In choosing the size of the area, I took into account the available evidence on its seismicity, seismotectonics, and seismogeodynamics.

Earthquake sources are shown in Fig. 1 in accordance with their size and spatial orientation. This representation is based on a legend that was previously proposed by the author and basically differs from the traditional abstract pointwise representation of earthquake epicenters: earthquake sources with $M \geq 7.0$ are mapped as ellipses with a realistic orientation of their major (l) and minor (w) axes. Their sizes and relative diameters of circles l' representing $M \leq 6.5$ earthquake sources are calculated by the formulas [Ulomov, 1974, 1999]

$$M \geq 6.5: \ \log l \ = \ 0.6M - 2.5;$$
$$\log w \ = \ 0.15M + 0.42; \qquad (1)$$
$$M < 6.5: \ \log l' \ = \ 0.24M - 0.16.$$

The seismic potential of the study region is high. The strongest earthquakes with magnitudes of about $M = 8.0$ and higher occurred on the southern Caspian coast in various years: $M = 8.1$, 856; $M = 8.0$, 958; $M = 7.8$,

1668; and $M = 7.9$, 1895. The recent largest seismic events within the study region were the destructive ($M = 7.4$) Rudbar earthquake of 1990 in northern Iran and the Balkhan ($M = 7.3$) earthquake of 2000 near the eastern Caspian coast in western Turkmenistan. (Here and below, the magnitude M means the M_s value determined from surface waves.)

The geodynamics and seismicity pattern of the study region, compressed by the Iranian continental plate in the south and by the Scythian-Turan continental plate in the northeast, are noticeably ordered. The symmetry of linear and arcuate structures whose axes are shown in Fig. 1 by broken lines is distinctly recognizable within the region. These are two parallel lineaments characterized by the largest earthquakes and a sine-like seismogenic structure exhibiting three bends with apexes at the Caucasus, Elburz, and Kopet Dag. The northern lineament extends along the Greater Caucasus, central Caspian Sea, and Kopet Dag, whereas the southern one traces sources of large earthquakes from the North Anatolian fault in the west to the Elburz mountainous structures and possibly extends farther to the east. All these structures are seismically most hazardous [Ulomov and Shumilina, 1999].

The South Caspian block located at the center of the study region has an oceanic lithosphere that is less pliable to geodynamic deformations and is virtually aseismic in its central part. Note that the northern edge of the Arabian plate in the west and the median Lut massif in the east of the Iranian plate are likely to be another two strong portions of the continental lithosphere that are largely responsible for the sine-like configuration of the seismicity pattern. The arrows in Fig. 1 show the movement directions of lithospheric plates and the interaction between the southern and northern Caspian geoblocks.

Figure 2 plots the year-averaged recurrence of $M \geq 4.0$ earthquakes that occurred within the entire study region (solid circles) and solely in its offshore area (open squares). Each plot is provided with its approximating linear equation (an exponent), obtained by the maximum likelihood method and enabling the calculation of the year-averaged flow of seismic events in a given magnitude interval.

The available information on the seismicity and seismic regime of the Caspian region is fairly comprehensive. The slopes of the recurrence plots b are normal and their values on land and sea virtually coincide. The yearly averages of the flow of seismic events N are well fitted by a log-linear (exponential) function. An exception is seismic events with $M = 7.0$ and 7.5 in the entire region and with $M = 6.0$ and 6.5 in its offshore area; this is quite natural, because higher-magnitude earthquakes occur much more often than could be expected from the ordinary linear extrapolation of recurrence plots to the right [Ulomov and Shumilina, 1999]. Higher recurrence rate intervals of large earthquakes are marked by broken lines. Note also that the seismic activity level in
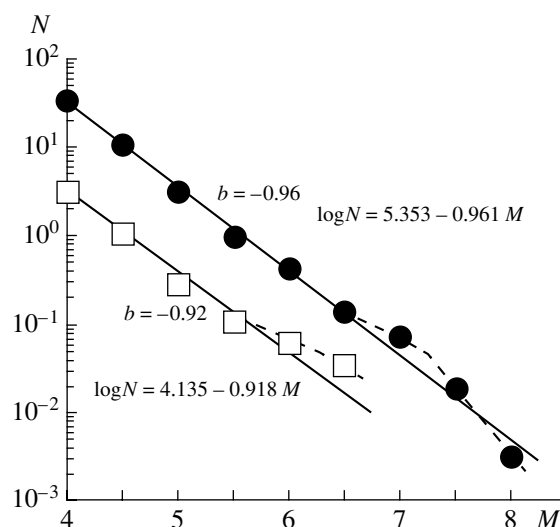
Fig. 2. Recurrence plots of earthquakes of various magnitudes in the study region (solid circles) and the Caspian Sea water area (open squares). N is the year-averaged number of events with magnitudes within the range $M \pm 0.2$ calculated with a magnitude step of 0.5, and b is the recurrence plot slope.

the Caspian water area is significantly lower compared to the entire study region, which is accounted for by both the smaller sea area and the specific seismogeodynamic features of the entire region.

The majority of seismic events throughout the study area have sources at depths of 10 to 15 km. However, as noted above, a characteristic feature of the seismicity in the region is the presence of deeper sources; they are usually confined to the linear and arcuate structures shown in Fig. 1 and are most frequent in the Caucasus, where their depths often exceed 75 km. Seismic sources with depths of up to 140 km are known on the Caspian segment of the Caucasus–Kopet Dag lineament. Similar to other well-pronounced linear and arcuate elements of the seismicity pattern, this zone is clearly traceable in maps showing the gradients of isostatic and other geophysical anomalies (Fig. 3).

The ophiolitic belt extending on both sides of the Caspian Sea is another factor favoring the subduction origin of the Caucasus–Kopet Dag zone. Within the central Caspian water area, this zone is traceable by the relatively large earthquakes of 1911 ($M = 6.4$), 1961 ($M = 6.0$), 1963 ($M = 6.2$), 1986 ($M = 6.2$), and 1989 ($M = 6.2$ and 6.3). Among the coastal events located on the same trace, the strongest were the Krasnovodsk earthquake of 1895 ($M = 7.9$) in western Turkmenistan and the earthquake of 1668 ($M = 7.8$), which occurred on the opposite Caspian coast.

SEISMOGEODYNAMIC MODEL OF THE REGION

The aforementioned correlation between local seismicity phenomena and anomalous variations in the Caspian Sea level indicates their common geodynamic origin, which is likely due to a specific deformation of the crust and the whole lithosphere in the region studied. The occurrence of seismic events with deep hypocenters is evidence of specific development of deep seismogenic processes involving the entire southern Caspian oceanic crust plunging into the upper mantle. As noted in [Ulomov *et al.*, 1999], anomalous varia-
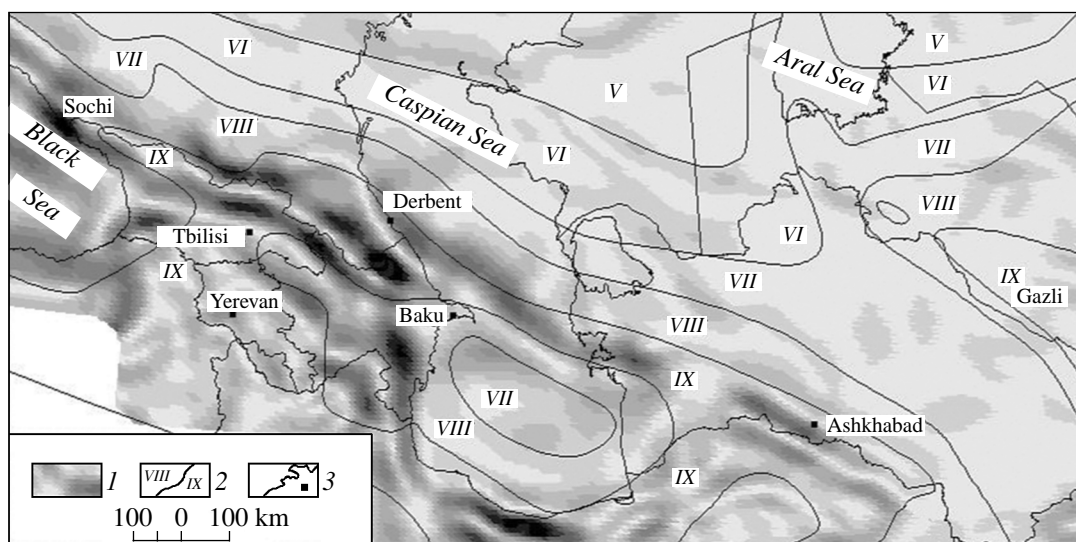

Fig. 3. General seismic zoning (OSR-97) map of the Caspian region: (*1*) gradients of isostatic anomalies (after the data of M.E. Artemyev and M.K. Kaban); (*2*) fragment of the OSR-97-A map showing seismic intensity zones (units of the MSK-64 scale, a 0.9 probability that the seismic intensity will not be exceeded for 50 years, and an average recurrence of one seismic event per 500 years) [Ulomov and Shumilina, 1999]; (*3*) national borders and towns.
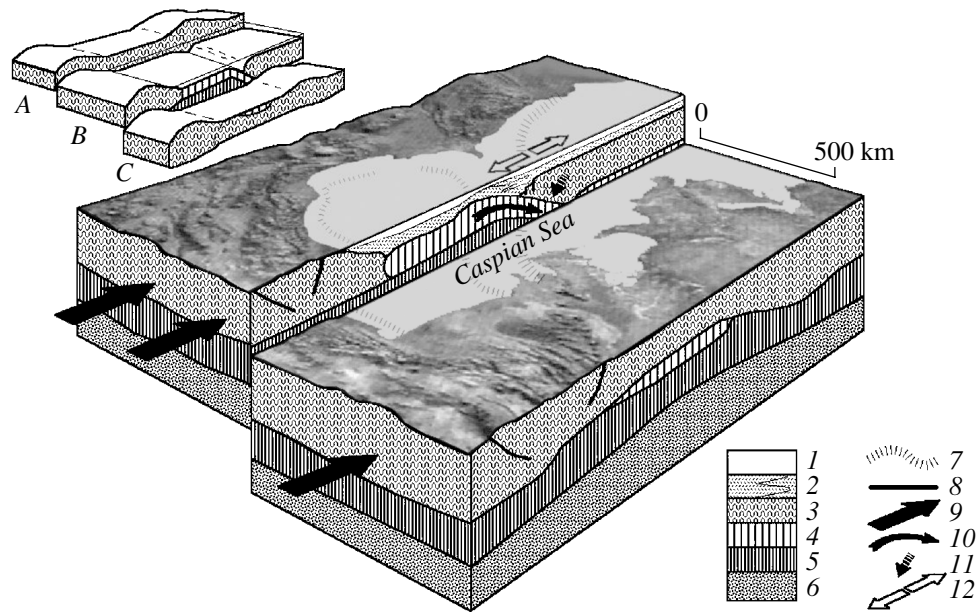
Fig. 4. A 3-D seismogeodynamic model of the Caspian region (the vertical scale is exaggerated): (*1*) water mass; (*2*) sedimentary sequence and faulted sediments in the central Caspian Sea; (*3*) continental crust; (*4*) oceanic crust relics; (*5*) subcrustal lithosphere; (*6*) asthenosphere; (*7*) maximum gradients of isostatic anomalies; (*8*) large tectonic faults; (*9*) direction of the pressure exerted by the Iranian and Arabian plates; (*10*) direction of the South Caspian lithosphere subduction under the Scythian-Turan plate; (*11*) movement direction of the North Caspian lithosphere entrained by subduction; (*12*) local subhorizontal extension in the bending North Caspian lithosphere. The upper picture schematically illustrates the dynamics of the (*A*) Caucasus–Talysh, (*B*) Elburz–Caspian, and (*C*) Kopet Dag–Turan blocks.

tions in the sea level are likely due to alternating slow bending deformations of the southern Caspian oceanic lithosphere and rapid dip-slip motions in the subduction zone.

The seismogeodynamic 3-D model of the Caspian region (Fig. 4) developed by the author is based on the examination of the spatiotemporal and energy patterns of seismicity and the deep structure and dynamics of the lithosphere, as well as on the analysis of other geophysical, geodetic, and geological evidence. The main features of the model are explained in Fig. 4. Three blocks of the model are shown separately in the upper left corner of the figure. The Caucasus–Talysh (*A*) and Kopet Dag–Turan (*C*) blocks are continental, whereas block *B* includes the Caspian Sea and Elburz mountainous structures. All three blocks experience in the south the geodynamic pressure of the Arabian and Iranian plates.

Under conditions of the submeridional compression, the blocks of the region are deformed and thicken, giving rise to mountainous structures. The southern Caspian crust was found to be the strongest and most resistant to folding. The pressure of the Elburz Mountains makes it descend under the continental crust of the Scythian-Turan plate in the central Caspian region across the entire Cheleken-Apsheron threshold. The continental crust involved in the motion along the subduction zone also experiences bending and related

extension in its upper part; these deformations are accommodated by slip motions of the normal faulting type. This is supported by the focal mechanisms of seismic sources in the subduction zone, which are normal faults, as distinct from adjacent continental areas [Balakina *et al.*, 1993]. In the seismogeodynamic model developed in the present paper, the direction of the slab motion does not change its sign and focal mechanisms in seismic sources remain virtually the same over time.

The subduction process consists of several successive stages schematically illustrated in Fig. 5 (from top to bottom). The horizontal compression and buildup of elastic stresses in the oceanic lithospheric plate (top of the figure) bend it upward (middle), displacing the sea water mass and raising the sea level. Upon reaching critical values of elastic bending, margins of this plate descend under the continental lithosphere, flattening the plate and thereby lowering the sea level (bottom of the figure). The descent of the margins can be implemented through both rapid seismic motions and slow creep.

To quantify the bending effect of the South Caspian lithospheric plate on the sea level, I perform the following simplest calculations. Let this plate (supposed to be strong enough) be modeled by a rectangular plane area with the sides *a* and *b* (Fig. 6). The pressure from the south (arrows in the top figure) displaces the frontal edge of the plate *b* in the horizontal direction by a value
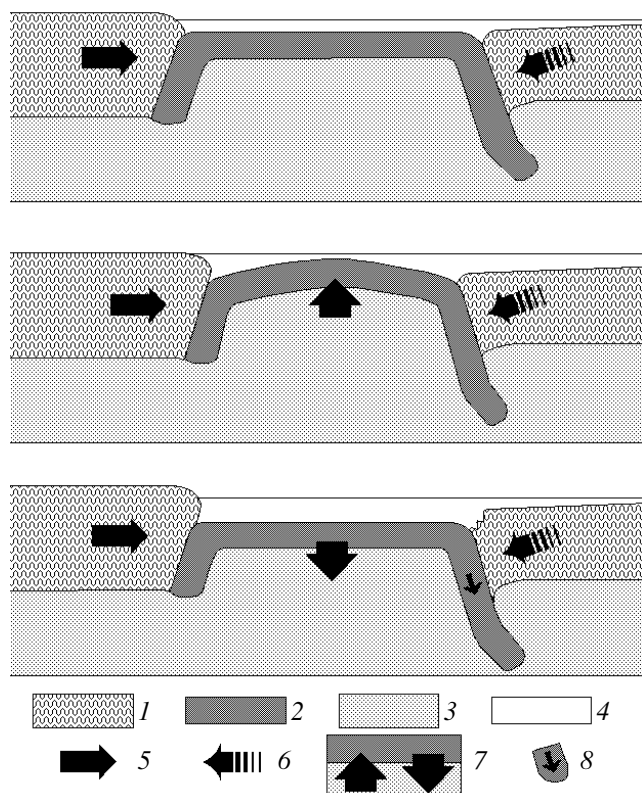
Fig. 5. Illustration of the mechanism of horizontal compression (top), bending (middle), and subsequent sinking of the South Caspian oceanic lithosphere: (*1*) continental lithosphere; (*2*) oceanic lithosphere; (*3*) upper mantle; (*4*) water mass; (*5*) direction of the Elburz push; (*6*) sinking direction of the bent North Caspian portion of the Scythian-Turan plate; (*7*) direction of bending and sinking of the South Caspian oceanic lithosphere; (*8*) sinking direction of the oceanic lithosphere in the subduction zone.
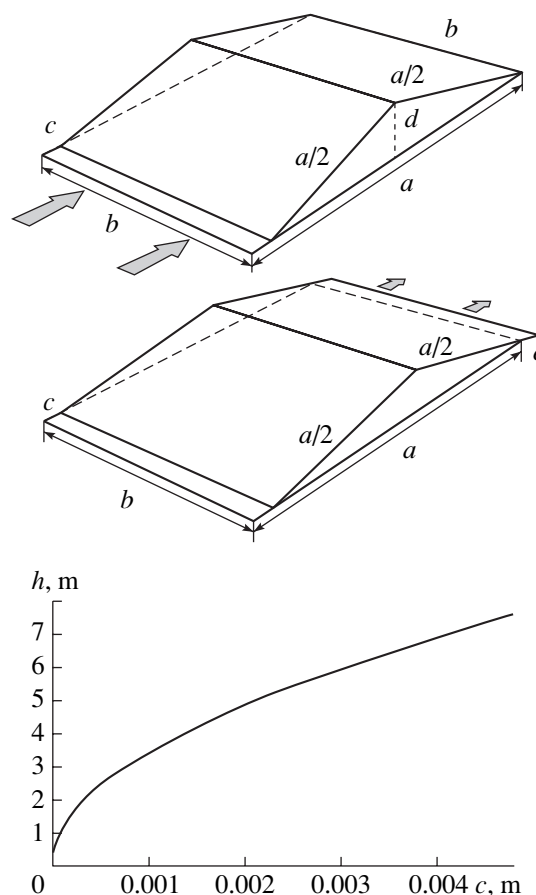

Fig. 6. Upper boundary deformation of the South Caspian oceanic lithosphere due to horizontal movements of its edges: *a* and *b* are the horizontal dimensions of the South Caspian plate, and *d* is the apex height of the broken line modeling the bending deformation. Top panel: horizontal displacement (*c*) of the southern edge of the plate (the opposite edge is fixed). Middle panel: subsequent displacement (*e*) of the opposite edge of the plate (arrows in the subduction zone) and the partial flattening of the plate. Lower panel: the height of the water level rise (*h*, in meters) throughout the sea surface as a function of *c*. For the rest of explanations, see the text.

c, whereas its northern edge remains immobile. Since the oceanic lithosphere is incompressible, the plane *ab* is bent. To a first approximation, this bend is described in our model as a broken line, with its central part uplifted by a value *d*; given very small *c* values and very large sizes of the area *ab*, this approximation is admissible. The incompressibility of the lithospheric plate also implies that each lateral edge of the bent surface is equal to *a*/2. Then, according to Fig. 6, the following expressions are readily obtained:

$$d = \frac{1}{2}\sqrt{c(2a-c)};$$

$$V = \frac{(a-c)bd}{2} = \frac{b(a-c)}{4}\sqrt{c(2a-c)}; \qquad (2)$$

$$h = \frac{V}{S} = \frac{(a-c)b}{4S}\sqrt{c(2a-c)},$$

where *V* is the volume bounded by the plane *ab* and the newly formed figure with faces *a*/2 and *b*, the height *d*, and the base of an area (*a* − *c*) *b* and *h* is the height of

the sea level rise throughout the sea surface *S* (not only in the southern Caspian Sea). Actually, *V* is the volume of the entire Caspian Sea water displaced by the newly formed configuration of the seafloor.

The model of the succeeding stage of the southern Caspian lithosphere dynamics is illustrated in the central picture of Fig. 6. The opposite edge of the plate *b* is now displaced by a value *e*, whereas its frontal edge displaced by the value *c* remains fixed. This process is accompanied by seismic activation and creep in the subduction zone, flattening of the plate, and the associated drop in the sea level. Finally, when the plane *ab* becomes flat due to an increase in the number and amplitudes of movements *e*, i.e., when $\sum e = c$, the plane *ab* as a whole is displaced northward. Such is the

model of the driving mechanism of the Caspian oceanic lithosphere that can completely sink in the subduction zone of the central Caspian Sea over a certain geological time interval.

Now, I take typically Caspian values of model parameters: $a = 400 \times 10^3$ m, $b = 450 \times 10^3$ m, and $S = 3.71 \times 10^{11}$ m². Then, setting $c = 10$ mm, the maximum amplitude of the sea level rise is $h = 10.8$ m. According to geodetic GPS data [Guliev *et al.*, 2002; Jackson *et al.*, 2002], the actual value of c in the Caspian region can be an order of magnitude smaller. However, even such values of horizontal movements of a perfectly rigid plate, amounting to very small fractions of a degree (the strains in the plate do not exceed 10^{-4}) result in relatively large variations in the sea level. As an illustration of this phenomenon, the sea level rise amplitude h is plotted in the lower part of Fig. 6 as a function of the horizontal displacement (c) of the southern Caspian lithosphere edge.

Undoubtedly, under real conditions, even a strong oceanic lithospheric plate is not a perfectly rigid body and experiences some deformations. Moreover, the sea coasts are not plumb, as is assumed in the first model approximation in Fig. 6, but are generally gently sloping. This primarily relates to the northern Caspian Sea, where a flood caused by a rise in the sea level is a significant, sometimes catastrophic, phenomenon. In principle, these and other factors can be accounted for, but this does not significantly change the relative estimates of h and c obtained above in terms of the simplest model. In other words, even insignificant displacements of the southern Caspian plate edge will result in substantial variations in the sea level.

SEISMIC REGIME AND SEA LEVEL VARIATIONS

The results presented below are based on a new methodological approach and additional seismological data. I address the sequences of earthquakes of various magnitudes that occurred within the study region (see Fig. 1). Figure 7 shows variations in the time intervals dT (in years) between earthquakes of various magnitudes that occurred within the study region over the period from 1830 through 2002. The curve of variations in the Caspian Sea level L is also shown in this figure. Earthquakes within magnitude intervals of 8.0 ± 0.2, 7.5 ± 0.2, 7.0 ± 0.2, 6.5 ± 0.2, and 6.0 ± 0.2 were considered. All seismic events are representative within the study area and in the time interval considered, and no evidence on the largest events that occurred over several centuries is missing.

The dT value is the time interval between successive seismic events in each of the sequences considered (in a given magnitude interval M). These values correspond to the width of histograms whose areas are proportional to such "delays" in the occurrence time of a current earthquake. The more frequent the earthquakes,

the closer to the abscissa axis the respective dT values and the smaller the amplitude and area of the histogram. Vice versa, longer delays increase the area and height of histograms. Evidently, if seismic events occurred uniformly in time, their occurrence moments would lie exactly on a horizontal line specified by the ordinate equal to the period of such a rhythm. The actual distribution of seismic events exhibits a regular variation caused by deep seismogeodynamic processes.

The ordinate scale L of the right-hand bottom plot relates to the variation curve of the Caspian Sea level. For the sake of comparison, this scale is reproduced in Fig. 6 for each sequence of earthquakes of various magnitudes. Seven categories of the sea level states can be considered. Three of them reflect a stable state of the level and its rise and drop. The other four characterize changes in these states (rise–drop and drop–rise) and changes in the rate (drop–drop and rise–rise). Less significant higher-frequency fluctuations of the sea level are not considered here. They are likely due to various endogenic and exogenic factors (climatic, hydrological, and others). Eliminating this high-frequency component, the curve L can be approximated by the broken line shown in Fig. 7.

The following time intervals are recognizable: (1) 1838–1855, a sea level drop; (2) 1855–1880, a rise at about the same rate; (3) 1880–1930, a relatively slow and long-term drop; (4) 1930–1940, a very rapid, relatively short, and intense (nearly 2 m) drop; (5) 1940–1978, a slow long-term drop; (6) 1978–1992, a very rapid, relatively short, and intense (nearly 2 m) rise; and (7) 1992–2002, a rapid drop. Along with these categories, two sign changes in the sea level behavior (drop–rise and rise–drop) are observed, and the drop rate changed two times.

Analysis of time intervals between successive earthquakes in relation to variations in the seismic regime and sea level shows that they are correlated.

In accordance with the seismogeodynamic model of the Caspian Sea described above, this relation is most distinct in the case of the largest seismic events. Thus, the Krasnovodsk $M = 7.9$ earthquake of 1895 (eastern coast of the Caspian Sea; see Fig. 1) occurred more than two centuries after a similar earthquake of 1668 on the opposite coast (in the town of Shemakha area in Azerbaijan) and was preceded by a short rise in the sea level (2). (Note that any reliable evidence on Caspian Sea variations before 1838 is unfortunately unavailable.) The Krasnovodsk earthquake, the most significant in the region, was followed by a long (nearly 100-year) interval of the Caspian Sea level drop including three stages (3–5) of variation in the rate of this process.

No less convincing is the sequence of $M = 7.5 \pm 0.2$ earthquakes that started, after a 150-year seismic quiescence, with the earthquake of 1930 that occurred west of the southern Caspian coast against the background of a relatively high sea level. It is noticeable that this
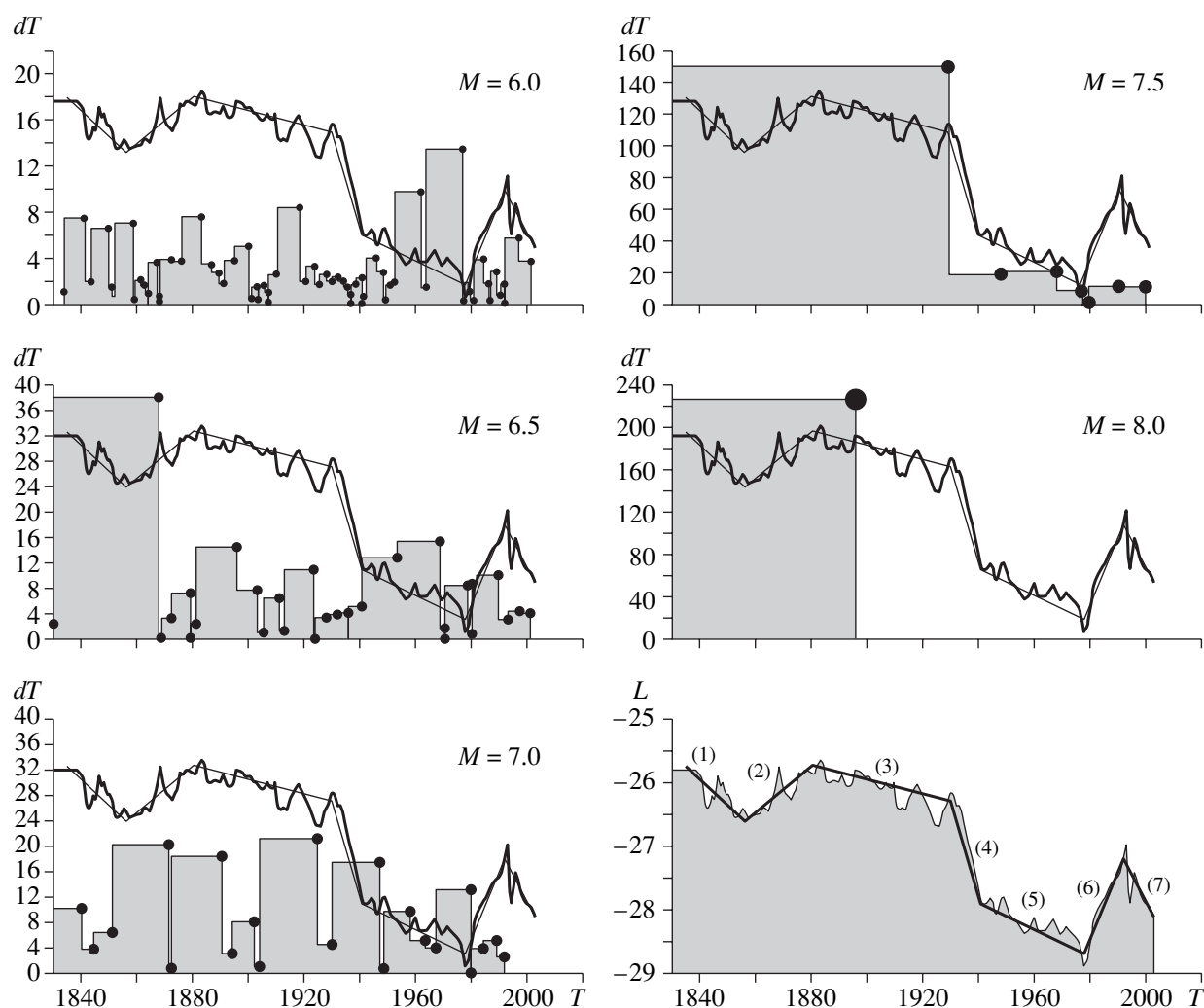
Fig. 7. Variations in the time intervals dT (in years) between successive seismic events (solid circles) of various magnitudes M and in the Caspian Sea level (L, in meters) during the time T (the years 1830–2001). (1)–(7) Are the sea level variation stages.

earthquake was followed by a series of shocks along the Derbent trench in the central Caspian water area, their sources being deepest in Caspian Sea; the largest of these shocks occurred in 1931 ($M = 6.2$, $H = 110$ km) and 1935 ($M = 6.3$, $H = 100$ km). All these events were followed by a substantially accelerated drop of the Caspian Sea level (stage 4). The seven largest earthquakes with $M = 7.5 \pm 0.2$ occurred at stages characterized by a slowdown in the sea level drop (stage (5)) and by sharp variations in the sea level (stages (6) and (7)). The time intervals between these events averaged about 10 years, which is a very high recurrence rate, taking into account that such events were not observed in this region for one and a half centuries. Their sources are emphasized in Fig. 1 by thicker contours and their occurrence years are given at the contours.

The earthquake of 1930 was followed by the Ashkhabad catastrophe of 1948. A similar earthquake in Iran occurred in the same structure south of Ashkhabad

in 1968 (i.e., after nearly the same time interval). Afterward, three earthquakes of the same rank took place in a very short time interval (1976–1979), coinciding with a sign change in variations of the sea level (the drop–rise stage) and its dramatic rise in 1978. The first occurred west of the Caspian Sea in 1976, and the other two (1978 and 1979), east of the sea, at nearly the same distance from the coast. The next two seismic events of the same rank separated by an interval of 10 years took place in the proximity of Caspian coasts. These were the destructive Rudbar, northern Iran earthquake of 1990 and the equally strong 2000 earthquake in offshoots of the Greater Balkhan Ridge in western Turkmenistan (see Fig. 1).

The final sign change of the rise–drop type took place immediately after the Rudbar earthquake, with the sea level drop being no less rapid. Presently, it is difficult to gain additional constraints on the relation between the sea level variations at stages (5)–(7) and

—

the last seven $M = 7.5 \pm 0.2$ earthquakes, apart from that the very high recurrence rate coincided in time with sharp sea level variations. However, it is noteworthy that the statistically mean distances δ_M (km) between the nearest sources of all seismic events with $M = 7.5 \pm 0.2$ that occurred from 1930 through 2000 along the seismogenic structures shown in Fig. 1 are consistent with the "standard" values previously obtained by the author in other seismically active regions of North Eurasia. The value δ_M also constrains the size (diameter) of the area involved in the preseismic process preceding an earthquake of the respective magnitude [Ulomov, 1987a, 1987b, 1993, 1998]:

$$\log \delta_M = 0.6M - 1.94. \qquad (3)$$

According to (3), an estimate $\delta_M = 363$ km is obtained for earthquakes with $M = 7.5$. Given a magnitude interval of $M = 7.5 \pm 0.2$, the range of δ_M values amounts to 275–480 km. Under the real conditions of the study region, the statistical mean of δ_M is 313 km with an rms deviation of $\sigma = \pm 93$ km, which yields a range of distances of 220–400 km, i.e., close to theoretical estimates. These calculations used distances between three sources along the southern lineament in the west of the study region and distances between four sources located east of the Caspian Sea along the northern lineament and its southeastern continuation along the arcuate structure.

Intricate seismogeodynamic and hydrogeodynamic processes in the Caspian region continue. Notwithstanding the very rapid rise in the sea level that started in 1978, its position is still much lower than its heights preceding not only the Krasnovodsk earthquake but also the Iranian earthquake of 1930. In line with the concept of preferable distances between epicenters (PDE) [Ulomov, 1987a, 1987b], the position of the potential source of the forthcoming $M = 7.5 \pm 0.2$ earthquake can be predicted with a fairly high probability. This source is likely to be located in the coastal zone of the southeastern part of the southern Caspian Sea coinciding, according to the PDE concept, with a "gap" that has not been filled since 856, when the largest ($M = 8.1$) historical earthquake occurred in this area. The northeastern Caucasus remains another zone of potential seismic hazard, as was repeatedly noted in [Ulomov, 1993, 1998; Ulomov *et al.*, 1999].

Since 1946, the sequence of $M = 7.0 \pm 0.2$ (see Fig. 7) earthquakes has been characterized, similar to that of $M = 7.5 \pm 0.2$, by a recurrence rate that is twice as high. This time period covers stages (5) and (6) of sea level variations. No earthquake of this rank has occurred during stage (7) as yet. Similar to the case of $M = 7.5 \pm 0.2$, no closer correlation between seismicity and sea level variations is recognizable, apart from the fact that the recurrence rate of events at stages (5) and (6) increased. More detailed calculations and analysis are required.

On the other hand, the sequences of seismic events with $M = 6.5 \pm 0.2$ and 6.0 ± 0.2 are similar in an appreciable decrease in the recurrence rate at stage (5) and its increase at stages (4) and (6) corresponding to rapid sea level variations. Also noticeable is a 38-year $M = 6.5$ quiescence (1830–1868), coinciding with the first period of a relatively low sea level (stages (1) and (2)), after which earthquakes of this rank occurred on average every 4–5 years.

Further examination of the correlation between seismogeodynamic and hydrogeodynamic processes should take into account earthquake source sizes and their distance from the Caspian Sea water area. For example, although earthquake sources of a relatively low rank can be very sensitive to small fluctuations of geodynamic stresses and strains in numerous small blocks, variations in the sea level will remain unaffected by such sources provided that they are far from the Caspian Sea water area.

ELEMENTS OF LONG-TERM PREDICTION

For the purpose of monitoring of seismogeodynamic processes and long-term prediction of strong earthquakes, the sequences of events with $M = 7.5 \pm 0.2$, 7.0 ± 0.2, and 6.5 ± 0.2 were used to construct cumulative plots of the number of earthquakes versus time shown in Fig. 8 (n is the order number of an event in each chronological sequence). The straight lines obtained by the least-squares method approximate the entire set of events in each sequence. The respective equations with pertinent correlation characteristics (R^2), standard deviations (SD), and predicted earthquake occurrence times (t_p) are presented in the inset. If seismic events occurred uniformly in time, they would all lie exactly on the approximating lines. Their real behavior, albeit stationary on a long-term scale, exhibits certain anomalies including those described in the preceding section and shown in Fig. 7. These are primarily the acceleration and slowdown periods of seismic processes. For comparing the seismic regime with variations in the Caspian Sea level, the plot of the latter is also presented in Fig. 8.

Evidently, the probability of an earthquake increases with increasing deviation of earthquake occurrence moments from their long-term averages predicted by the approximating line. This is the essence of the simplest prediction scheme for earthquakes of a given magnitude. As seen, slowdown periods can last 30 to 40 years, after which the earthquake recurrence rate rapidly increases. Such time intervals of relative seismic quiescence can be 1930–1970 for $M = 7.5 \pm 0.2$ and 1940–1970 for $M = 6.5 \pm 0.2$. As regards seismic events with $M = 7.0 \pm 0.2$, their very rapid 10-year development was followed by a period of relative quiescence that started in 1990 after the Rudbar earthquake. Presently, this curve deviates from the approximating line by about 20 years. A similar situation took place in the first half of the 20th century, when strong
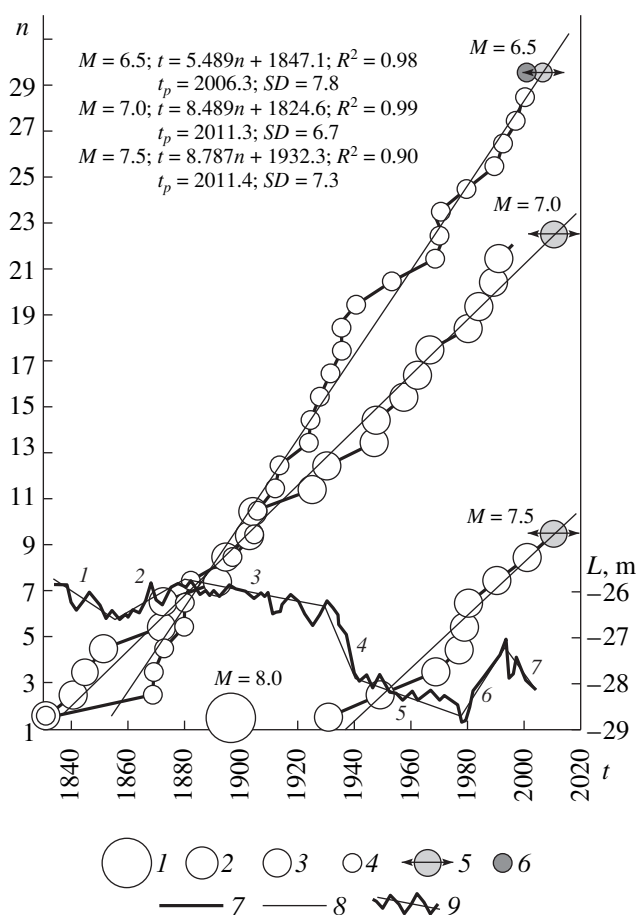
Fig. 8. Sequences of seismic events of various magnitudes and the long-term prediction of strong earthquakes in the study region (n is the order number of an event and t is the observation time (in years)): (*1*) $M = 8.0 \pm 0.2$; (*2*) $M = 7.5 \pm 0.2$; (*3*) $M = 7.0 \pm 0.2$; (*4*) $M = 6.5 \pm 0.2$; (*5*) predicted earthquakes (arrows are standard deviations *SD* from the average times t_p); (*6*) the $M = 6.5$ earthquake that occurred in northern Iran on June 22, 2002 (after the construction of these plots); (*7*) smooth interpolation of the initial data; (*8*) long-term linear trend; (*9*) curve and stages of Caspian Sea level variations. For the rest of explanations, see the text.

earthquakes of this rank occurred about 20 years after such slowdowns in the accumulation of seismic events.

Thus, using cumulative plots of seismic events and long-term average characteristics of the seismic regime, occurrence time intervals of current earthquakes of a given magnitude can be predicted with a certain probability. Importantly, the occurrence time moment of such events in the plane *tn* has only one degree of freedom, because each event can only shift in the horizontal direction without deviating from the level corresponding to its current order number. This allows one to predict, with a high probability, time intervals of enhanced seismic hazard. Thus, an $M = 7.5 \pm 0.2$ earthquake (no. 9) should occur in the study region in the period from 2004 to 2019 with an average date of 2011.4 and the standard deviation $SD = \pm 7.3$. As noted in the preceding section, its source will probably

be located either southeast of the Caspian Sea or in the northeastern Caucasus [Ulomov, 1993; Ulomov *et al.*, 1999]. An $M = 7.0 \pm 0.2$ earthquake (no. 22) can occur during the years from 2004 to 2018. However, judging from the accelerated development of previous events, there are reasons to believe that it is more likely to occur much earlier, i.e., before 2004.

An example of the confirmed prediction of an $M = 6.5$ event is the recent destructive earthquake of June 22, 2002 in northern Iran within the study region under consideration (see Fig. 1). This event was not used in our calculations. However, it lies within the prediction interval of 1998 to 2014 indicating a very high probability of such an earthquake to occur.

CONCLUSION

Based on the analysis of the deep structure of the crust and the entire lithosphere, as well as on the study of the fine structure of regional seismicity and recent tectonic movements, a seismogeodynamic model of the Caspian region is proposed. According to this model, a seismic activation is preceded by a rise in the seafloor of the South Caspian basin and the appearance of "excessive" sea water, and vice versa, a general drop of the sea level follows large earthquakes and the sinking of the related crustal blocks in the subduction zone. Numerical estimates are obtained for geodynamic strains in the southern Caspian oceanic lithosphere responsible for the accumulation of elastic stresses and preseismic processes of local earthquakes.

The examination of variations in the seismic regime and the Caspian Sea level revealed regular patterns supporting a common deep origin of both phenomena. Being isolated from the ocean, the Caspian basin is shown to be sensitive to the smallest deformations of the lithosphere and is a specific indicator of the local geodynamics and seismicity. The joint study of seismogeodynamic and hydrogeodynamic phenomena provides new possibilities for the long-term prediction of strong earthquakes in the Caspian region. The analysis revealed that large ($M = 7.0 \pm 0.2$) earthquakes can occur in the study region in the near future. The position of their sources is to be determined by the analysis of the migration of seismogeodynamic processes and the identification of potentially hazardous areas of seismogenic structures using, among others, *GPS* methods.

Finally, it is interesting to recall to the reader that, according to ancient Persian and Arabian maps and written sources, the Caspian Sea in the historical past consisted of two separate reservoirs separated by a narrow isthmus that connected the eastern and western coasts of the contemporary sea and was a part of the famous Silk Route. This isthmus was destroyed over a very short time period due to a geological catastrophe unknown to us; presently, its relics can only be found on the Caspian seafloor and it is traceable by a chain of preserved islands extending along the Cheleken-Apsh-

eron threshold. Apparently, the same geological cataclysm changed the course of the Amu Darya River, which once flowed into the Caspian Sea in the seismogeodynamically most active area.

ACKNOWLEDGMENTS

REFERENCES

Ambraseys, N.N. and Melville, C.P., *A History of Persian Earthquakes*, Cambr. Univ. Press, 1982.

Balakina, L.M., Zakharova, A.I., *et al.*, Focal Mechanisms of Strong Crustal Earthquakes of 1927–1991 in North Eurasia, *Seismichnost' i seismicheskoe raionirovanie Severnoi Evrazii* (Seismicity and Seismic Regionalization of North Eurasia), 1993, vol. 1, pp. 123–131.

Baranova, E.P., Kosminskaya, I.P., and Pavlenkova, N.I., Results of Reinterpreting DSS Data from the Southern Caspian Sea, *Geofiz. Zh.,* 1990, vol. 12, no. 5, pp. 60–67.

Dotsenko, S.F., Kuzin, I.P., Levin, B.V., and Solovieva, O.N., Prognostic Estimates of Tsunami Heights in the Caspian Sea, *Morsk. Gidrofiz. Zh.,* 2001, no. 6, pp. 3–13.

Dotsenko, S., Kuzin, I., Levin, B., and Solovieva, O., Tsunami in the Caspian Sea: Historical Events, Numerical Modeling, *Local Tsunami Warning and Mitigation*, Petropavlovsk-Kamchatski, 2002, p. 16.

Dotsenko, S.F., Kuzin, I.P., Levin, B.V., and Solovieva, O.N., Possible Tsunami Implications of Seismic Sources in the Caspian Sea, *Izvestiya, Phys. Solid Earth*, 2003, vol. 39, pp. 308–314.

Gadzhiev, A.I. and Popkov, V.I., Structure of the Sedimentary Cover in the Central Caspian Sea, *Geotektonika*, 1988, no. 6, pp. 101–112.

Galperin, E.I., Kosminskaya, I.P., and Krakshina, R.M., Main Characteristics of Deep Waves in the Central Caspian Sea from DSS Data, *Glubinnoe seismicheskoe zondirovanie zemnoi kory v SSSR* (Deep Seismic Sounding of the Crust in the USSR), Leningrad: Gostoptekhizdat, 1962, pp. 227–250.

Gasanov, I.S., Andreev, L.I., Gasanov, G.Yu., *et al.*, *Razlomy akvatorii Srednego Kaspiya* (Faults in the Central Caspian Sea), VINITI, 1982.

Golubov, B.N., Novikov, V.L., and Shlesinger, A.E., Processes Controlling the Formation of Caspian Sea Water Mass and Variations in Its Level, *Dokl. Akad. Nauk SSSR*, 1998, vol. 358, no. 4, pp. 538–542.

Guliev, I.S., Kadirov, F.A., Reilinger, *et al.*, Active Tectonics of Azerbaijan from Geodetic, Gravity, and Seismic Data, *Dokl. Akad. Nauk,* 2002, vol. 382, no. 6, pp. 812–815.

Ivanova, T.P. and Trifonov, V.G., Seismotectonics and Recent Variations in the Caspian Sea Level, *Geotektonika*, 2002, no. 2, pp. 27–42.

Jackson, J., Priestley, K., Allen, M., and Berberian, M., Active Tectonics of the South Caspian Basin, *Geophys. J. Int.*, 2002, vol. 148, pp. 214–245.

Kaban, M.K., Artemyev, M.E., Karaev, D.I., *et al.*, Deep Structure and Geodynamics of Tectonic Structures in Turkmenistan and Adjacent Areas from Gravity Data, *Geotektonika*, 1998, no. 4, pp. 81–89.

Lavrushin, Yu.A., Leonov, Yu.G., and Lilienberg, D.A., Main Directions and Results of Studying the Effect of Geological Factors on the Caspian Sea Level Variations, *Global'nye izmeneniya prirodnoi sredy* (Global Environmental Variations), Novosibirsk: SO RAN, Filial "GEO," 2001, pp. 105–130.

Leonov, Yu.G., Gushchenko, O.I., Kopp, M.L., *et al.*, Relationships between the Cenozoic Stress-Strain States in the Caucasian Sector of the Alpine Belt and in Its Adjacent Northern Platform Area, *Geotektonika*, 2001, no. 1, pp. 36–59.

Lilienberg, D.A., New Approaches to the Recent Endogenic Dynamics of the Caspian Region and Problems of Its Monitoring, *Izv. Ross. Akad. Nauk, Ser. Geogr.,* 1994, no. 2, pp. 16–36.

Panakhi, B.M. and Rakhmanov, R.R., Seismicity of Mud Volcanism Areas, *Prognoz i kontrol' geodinamicheskoi i geoekologicheskoi obstanovok v regione Kaspiiskogo morya v svyazi s razvitiem neftegazovogo kompleksa* (Prediction and Monitoring of Geodynamic and Geoecological Settings in the Caspian Sea Region with Reference to the Development of the Oil-and-Gas Complex), Moscow: Nauchnyi Mir, 2000, pp. 111–126.

Shilo, N.A., The Origin of the Caspian Sea Level Fluctuations, *Dokl. Akad. Nauk SSSR*, 1989, vol. 305, no. 2, pp. 412–416.

Shilo, N.A. and Krivoshei, M.I., Relation between Caspian Sea Level Variations and Crustal Stresses, *Vestn. Akad. Nauk SSSR*, 1989, no. 6, pp. 83–90.

Ulomov, V.I., *Dinamika zemnoi kory Srednei Azii i prognoz zemletryasenii* (Dynamics of the Central Asia Crust and the Earthquake Prediction), Tashkent: FAN, 1974.

Ulomov, V.I., On the Size Relations between Sources and Earthquake Preparation areas, *Dokl. Akad. Nauk UzSSR,* 1987a, no. 9, pp. 39–40.

Ulomov, V.I., A Lattice Model of Source Seismicity and the Seismic Hazard Prediction, *Uzb. Geolog. Zh.,* 1987b, no. 6, pp. 20–25.

Ulomov, V.I., Global Ordering of Seismogeodynamic Structures and Some Aspects of Seismic Zoning and Long-Term Prediction of Earthquakes, *Seismichnost' i seismicheskoe raionirovanie Severnoi Evrazii* (Seismicity and Seismic Regionalization of North Eurasia), Moscow: IFZ RAN, 1993, vol. 1, pp. 24–44.

Ulomov, V.I., Interregional Working Meeting "Methodology and Algorithms in Studies of Regional Seismicity and Seismic Hazard Assessment in the Crimea–Caucasus–Kopet Dag Region," *Fiz. Zemli,* 1995, no. 3, pp. 92–96.

Ulomov, V.I., On the Identification and Seismological Parameterization of Earthquake Source Zones. The Caucasus and Adjacent Area, *Historical and Prehistorical Earthquakes in the Caucasus. NATO ASI. Series 2: Environment; vol. 28, ILP Publication no. 333*, Dordrecht: Kluwer, 1997, pp. 503–522.

Ulomov, V.I., Focal Zones of Earthquakes Modeled in Terms of the Lattice Regularization, *Izvestiya, Phys. Solid Earth*, 1998, vol. 34, pp. 717–733.

Ulomov, V.I., Seismogeodynamics and Seismic Zoning of North Eurasia, *Vulkanol. Seismol.*, 1999, nos. 4–5, pp. 6–22.

Ulomov, V.I., Seismic Menace in Russia, *Science in Russia*, 2001, no. 6, pp. 18–25.

Ulomov, V.I. and Shumilina, L.S., *Komplekt kart obshchego seismicheskogo raionirovaniya territorii Rossiiskoi Federatsii–OSR-97. Masshtab 1:8 000 000. Ob"yasnitel'naya zapiska i spisok gorodov i naselennykh punktov, raspolozhennykh v seismoopasnykh raionakh (A Set of General Seismic Zoning Maps (OSR-97), 1:8 000 000. Explanatory Note and the List of Towns and Townships Located in Seismically Hazardous Zones), Moscow: OIFZ, 1999.

Ulomov, V.I., Polyakova, T.P., and Medvedeva, N.S., Seismogeodynamics of the Caspian Sea Region, *Izvestiya, Phys. Solid Earth*, 1999, vol. 35, pp. 1036–1042.

Ulomov, V.I., Polyakova, T.P., and Medvedeva, N.S., On the Long-Term Prediction of Strong Earthquakes in Central Asia and the Black Sea–Caspian Region, *Izvestiya, Phys. Solid Earth*, 2002, vol. 38, pp. 276–290.

Vdovykin, G.P., Caspian Sea Level Variations in Relation to Neotectonic Movements, *Dokl. Akad. Nauk SSSR*, 1990, vol. 310, no. 3, pp. 673–675.